Development of an enhanced online tritium monitoring system using plastic scintillation fiber array*

Wen-Yu Cheng,[1,2] Ke Deng,[1] You-Shi Zeng,[1] Wei Liu,[1,2] and Qin Zhang[1,†]

[1]*Shanghai Institute of Applied Physics, Chinese Academy of Sciences, Shanghai 201800, China*
[2]*University of Chinese Academy of Sciences, Beijing 100049, China*

Tritium, a radioactive nuclide discharged by nuclear power plants, poses challenges for removal. Continuous online monitoring of tritium in water is crucial for real-time radiation data, given its predominant existence in the environment as water. This paper presents the design, simulation, and development of a tritium monitoring device utilizing a plastic scintillation fiber (PSF) array. Experimental validation confirmed the device's detection efficiency and minimum detectable activity. The recorded detection efficiency of the device is 1.6×10^{-3}, which exceeds the theoretically simulated value of 4×10^{-4} by four times. Without shielding, the device can achieve a minimum detectable activity of $3165\,\mathrm{Bq\,L^{-1}}$ over a 1600-second measurement duration. According to simulation and experimental results, enhancing detection efficiency is possible by increasing the number and length of PSFs and implementing rigorous shielding measures. Additionally, reducing the diameter of PSFs can also improve detection efficiency. The minimum detectable activity of the device can be further reduced using the aforementioned methods.

Keywords: Tritium; Plastic scintillating fiber array; Detector

I. INTRODUCTION

Tritium, the radioactive isotope of hydrogen, plays a unique role in nuclear physics and engineering due to its pure β-decay, emitting β rays with a maximum energy of $18.6\,\mathrm{keV}$ and an average energy of $5.7\,\mathrm{keV}$ during decay. With a half-life of 12.32 years [1], tritium can persist in the environment for an extended period, posing internal radiation hazards to humans upon ingestion. Currently, nuclear power plants serve as the primary source of tritium in the environment, emitting tritiated water (HTO) as the primary liquid emission [2, 3]. This tritium-contaminated water can enter the human body through ingestion or absorption, posing significant threats to human life and health [4–8]. Once released into the environment, tritium can substitute for hydrogen and enter the water and organic material cycles. Major news stories, particularly regarding the challenging issue of Fukushima water, have been repeatedly reported and shared, leading to extensive discussions among scholars, regulatory agencies, power plant operators, and the general public [9]. This heightened awareness has further fueled attention to the treatment of tritium-contaminated water and its associated environmental and health impacts. Offline monitoring fails to promptly reflect changes in tritium activity in water, potentially resulting in the failure to implement emergency measures during a crisis. Therefore, online measurement of tritium in water sources such as wastewater and drinking water is necessary to ensure the safety of the biological environment. By implementing online tritium monitoring, scientists and engineers can rapidly detect any increase in tritium activity and take immediate action to mitigate the potential risks posed by tritium contamination.

Liquid scintillation counting is an excellent method for measuring tritium in water [10–13]. However, the scintillator becomes contaminated with tritium, leading to the generation of organic solvent waste. This necessitates sample treatment for tritium measurement, a process that typically takes at least one day to complete, making it unsuitable for rapid water sample measurement [14–17]. Such batch processing monitoring might temporarily miss high tritium effluent. Therefore, continuous measurement monitoring is required to gain public confidence in tritium release. Additionally, a detection method that does not involve organic solvents would mitigate the waste disposal issue. Some researchers utilize small solid scintillation particles for detection. The principle of this method closely resembles that of the liquid scintillation counting method, hence it shares similar drawbacks. Contamination of the scintillation material occurs during the measurement process, rendering it non-reusable and incurring high costs. The measurement necessitates a specific duration for the sample preparation process. Currently, ongoing studies on online tritium monitoring in water show that the detectors used have minimum detectable activity ranging from 1×10^4 to $1 \times 10^6\,\mathrm{Bq\,L^{-1}}$ [18–23].

Plastic scintillation fiber (PSF) emerges as a promising solution for scientific investigations [18, 24–26], owing to its remarkable properties. Its inherent characteristics, such as a sizable effective detection volume and stability, designate it as an optimal medium for detection purposes. To bolster detection efficiency further, plastic scintillation fibers can be strategically augmented in quantity. A notable advantage of utilizing plastic scintillation fibers lies in their non-reactive nature and insolubility in water. These attributes render them highly suitable for repeated utilization, promoting sustainability and cost-effectiveness. As a result, this approach proves exceptionally well-suited for the development of online tritium monitoring systems specifically designed for water environ-

* This work was supported by the Young Potential Program of the Shanghai Institute of Applied Physics, Chinese Academy of Sciences
.; Shanghai Rising-Star Program, China (No. 22YF1457800);
The Chinese Academy of Sciences Youth Education Fund Program (No. E2292502);
Gansu Major Scientific and Technological Special Project under Grant (No.23ZDGH001).

† Corresponding author: zhangqin91@sinap.ac.cn

ments. The integration of this innovative material empowers researchers to reliably and efficiently monitor tritium levels in water sources, ensuring the preservation and safety of our aquatic ecosystems.

This study utilized the Monte Carlo simulation tool Geant4 to design the plastic scintillation fiber array and assess its impact on detector efficiency [27–30]. To align with experimental conditions, parameters such as the number, length, and diameter of the PSFs were optimized, followed by the structural design of the array. The aim was to maximize the detection volume, leading to the estimation of the theoretical detection efficiency. After completing the simulation, a detection system was developed and subjected to testing. Signal analysis and algorithm optimization were performed to enhance the system's performance. The detection efficiency and minimum detectable activity for tritium water sample calibration were evaluated, comparing and interpreting both the simulation results and experimental findings. Based on the outcomes, potential optimizations and advancements for the equipment were identified. Plans were formulated for the practical application of the detection system, considering the insights gained from the simulation and experimental phases. This comprehensive approach aimed to improve the overall effectiveness and applicability of the detection system for tritium measurement in water samples.

II. SIMULATION ANALYSIS

To determine the detection efficiency of the plastic scintillation fiber array for tritium detection in water, we employed a comprehensive computational approach. We utilized the widely acclaimed Monte Carlo simulation software, Geant4, for meticulous modeling and precise calculations, ensuring the validity and reliability of our results. Through this rigorous methodology, we distinctly illustrated the behavior of beta rays emitted from tritium decay within water, specifically highlighting their transmission depth. Our analysis revealed that these beta rays have a transmission depth of approximately 5 microns, aligning precisely with existing scientific literature [1, 3, 13, 21, 31]. The consistency observed between our simulation results and previous research further validates the accuracy and credibility of our computational model.Furthermore, we applied the same simulation methodology to investigate the range of tritium within the outer cladding of the plastic scintillation fiber. The simulation results, visually represented in Fig. 1, unequivocally indicate that the range of tritium within the outer cladding is less than ten microns. Conventional PSF structures consist of inner scintillation and outer cladding, with the latter typically being tens of microns thicker than the transmission depth of beta rays within it. Due to the low beta decay energy emitted by tritium decay, it cannot penetrate the outer cladding. Therefore, removing the outer cladding is necessary to enable direct entry of beta rays into the inner scintillation region. We utilized the PSF with the cladding structure removed in the subsequent simulations and experiments.

In Fig. 2, (a) depicts the foundational model of a detector utilizing plastic scintillating fibers (PSF) without cladding, implemented on the Geant4 simulation platform. This model comprises PSFs, a water layer serving as the radiation source, a reflector layer providing both reflection and shielding, and photocathodes positioned on both ends of the detector. The photon transport process is illustrated in (a), showing that the detector functions by depositing the energy from beta rays into the water layer, which then generates scintillation photons within the PSF. These scintillation photons propagate through the PSF fibers, ultimately reaching the photocathode of photomultiplier tubes (PMTs) located on both ends of the detector. The PMTs are responsible for converting these optical signals into electrical signals, facilitating signal processing and data analysis.

The properties of PSF, including its refractive index (1.58), density ($1.03\,\mathrm{g\,cm^{-3}}$), hydrocarbon ratio (1:1.1), decay time ($2.3\,\mathrm{ns}$), scintillation photon decay length ($2.00\,\mathrm{m}$), and max-

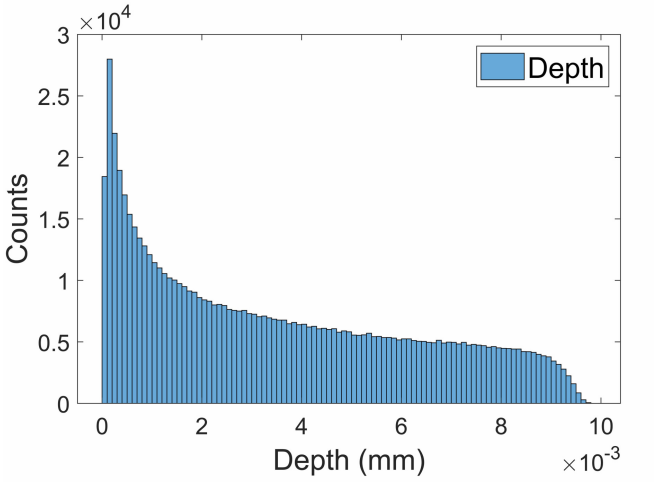

Fig. 1. Transmission depth of beta rays emitted by tritium decay in the outer cladding of PSF.

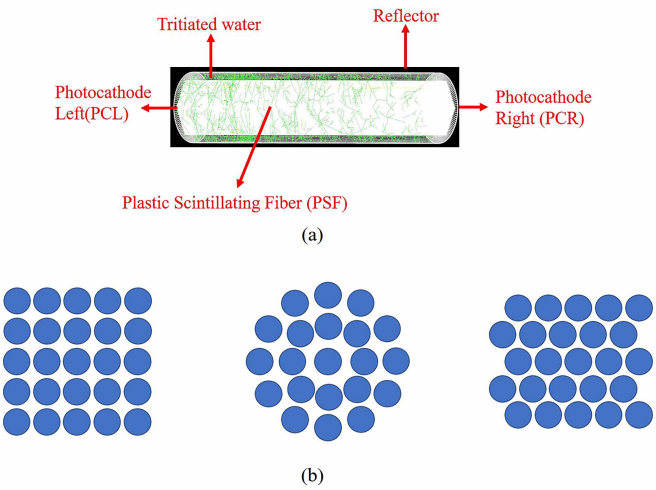

Fig. 2. Overview of the simulation model: (a) the model structure, (b) the probe array structure.

imum emission wave length (430 nm), are obtained from the Geant4 NIST database G4_POLYSTYRENE. The photon yield of $8400\,\mathrm{MeV}^{-1}$ is applied, considering possible nonlinearities at low energy. In the simulation, the reflective layer is designed with optical properties similar to those of a smooth, totally reflecting mirror, enabling efficient collection of scintillation photons. The radioactive source utilized is a tritium beta spectrum, uniformly distributed in space and emitting isotropic radiation. To ensure the convergence and reliability of our simulation results, an extensive number of particles, specifically $1 \times 10^9\ \mathrm{L}^{-1}$, are released by the specific volume of the radioactive source, enhancing statistical accuracy and reducing uncertainties in results.

In Fig. 2 (b), the configurations are as follows: the first is a square arrangement structure, the second is a circular arrangement, and the last is a hexagonal dense packing arrangement structure. The simulation results indicate that the hexagonal dense packing arrangement achieves significantly higher filling efficiency compared to the other two methods. Consequently, increasing the number of PSFs in the cylindrical detection chamber enhances detection volume and efficiency. Furthermore, each PSF has a detection range of less than 5 microns, and a spacing of 0.1 millimeters effectively detects all PSFs. Therefore, the PSF array is constructed using a hexagonal dense packing arrangement in this simulation.

The PSFs in this simulation had a diameter of 1 millimeter and length of 100 millimeters, with an interval between each PSF of 0.1 millimeters, and the diameter of the detection chamber was 22 millimeters. In Fig. 3 (a) presents the simulation results of the detection efficiency of the entire detection system under the given conditions; the overall detection performance of an array consisting of plastic scintillating fibers with matching radii within a detection chamber of identical radius is positively correlated with the number of PSFs utilized. This is because increasing the number of PSFs simultaneously expands the detection volume and reduces the volume of tritiated water. Assuming that the other conditions remain constant, an increase in the volume ratio directly increases the detection efficiency. Thus, to enhance the detection performance and efficiency of the detector, it is essential to maximize the number of PSFs in the detection array.

In Fig. 3 (b), the photon number distribution from the photomultiplier photocathodes is depicted at various PSF lengths, representing the energy spectrum derived from tritium measurements. It's important to note that the length of the PSF affects both the absorption of photons by water and the PSF itself, resulting in a decrease in the number of photons reaching the photocathode of the photomultiplier tube. Consequently, this reduction impacts the overall distribution of energy spectra exhibited by the photons. However, increasing the length of the PSF directly enhances the detection volume of the array, thereby improving the detection performance of the detector. Therefore, the influence of PSF length on detection efficiency should not be overlooked, and optimizing both the length and quantity of PSFs is crucial for enhancing the efficiency of the entire system.

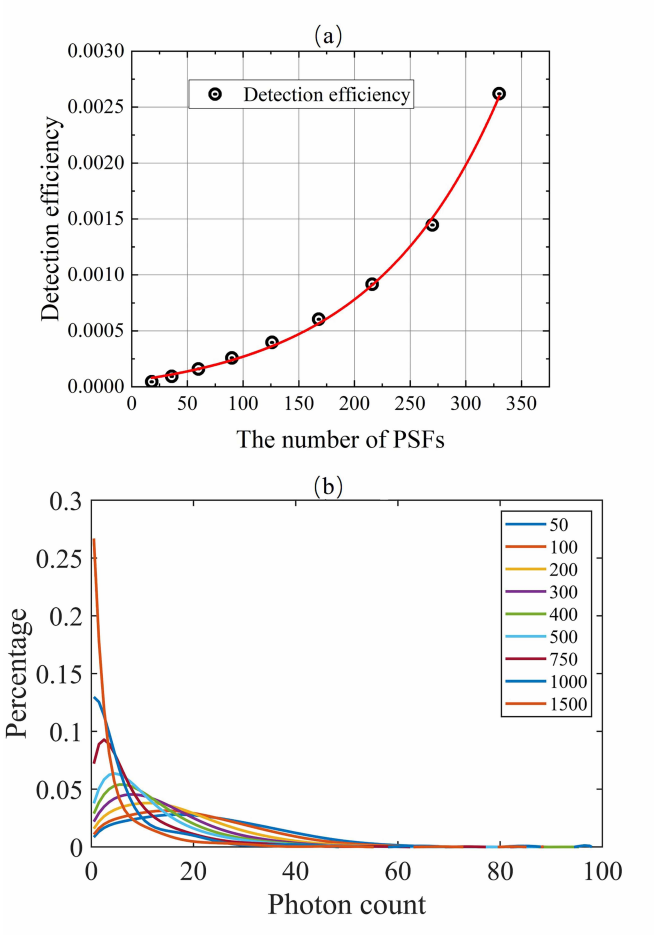

Fig. 3. Simulation results: (a) relation of different numbers of PSFs to detection efficiency, (b) influence of different lengths of PSF of photon distribution.

III. SYSTEM COMPOSITION

A. Detection structure

Fig. 4 (a) presents a comprehensive structural diagram of the detector system, offering clarity on its fundamental configuration. The system operates as follows: The target sample is introduced directly into the detection chamber through an injection port, pump, and flowmeter. Once inside the detection chamber, the sample undergoes a measurement process of specific duration. The detector functions by transferring energy from beta rays within the aqueous medium to plastic scintillating fibers, leading to the emission of scintillation photons. These photons then travel through the plastic scintillation fiber array and water medium, ultimately reaching the photomultiplier tubes, where they are converted into electrical signals. These signals undergo further processing to derive the desired measurement outcomes. After the measurement process is complete, the sample is discharged from the detection chamber and guided through a pipeline and flowmeter to a waste liquid tank for proper disposal.

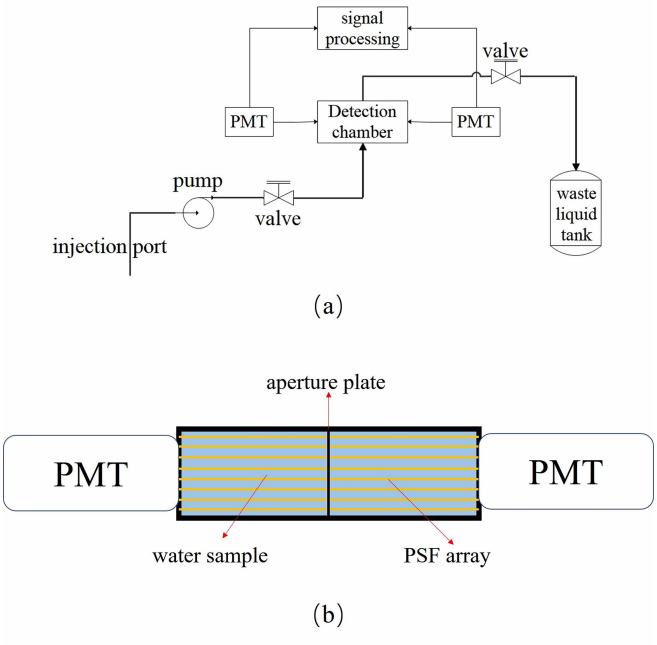

Fig. 4. Design of the system and detector: (a) Design of the system, (b) Design of the detector.

Fig. 4 (b) presents a detailed illustration of the probe chamber's structural arrangement. The plastic scintillation fiber array is positioned within the probe chamber using a grid system, ensuring that the PSFs' ends are close to the probe window. This placement minimizes water sample retention in the central region of the chamber. An airtight connection between the photomultiplier tubes and the probe is established using optical silicone. Additionally, the tubes are precisely aligned at both ends, aligning them with the chamber's geometric center. Efforts are made to direct the flow of water samples toward the lower end of the detection chamber to facilitate their exit from the upper end. Maintaining a predominantly horizontal flow is crucial to prevent bubble formation and potential interference within the chamber.

B. Signal analysis

The LeCroy-640Zi oscilloscope is an indispensable tool in our signal analysis process, especially after assembling the device under study. It utilizes continuous sampling over 1600 s to thoroughly analyze the detector's signals.

Our experimental setup involves the decay of tritiated water, which emits low-energy β-rays that interact with the plastic scintillator. However, due to limited energy transfer, fewer scintillation photons are produced, reducing the probability of simultaneous detection by the photomultiplier tubes located at both ends of the scintillator. Additionally, the quantum efficiency of the PMTs is diminished in these circumstances, resulting in relatively small amplitude signals that can be easily overshadowed by the inherent dark current noise in the PMTs. To address this issue, our system employs two PMTs for coincidental measurements at both ends of the plastic scintillator. Assuming that the dark current is randomly generated and that the scintillation photons propagate simultaneously towards both ends, we expect the photons to coincidentally reach the photocathode of each PMT and be detected. This approach ensures accurate capture of genuine coincidence signals while effectively suppressing the influence of interspersed dark-current noise [32, 33].

However, simultaneous detection of the dark current generated by both PMTs by their respective photocathodes can lead to false coincidence events. Long-term experiments should be conducted to assess the effect of these false coincidences on measurement results. Based on the observed curve and the relationship between coincidence counting and dark current during our experiments, we adjusted the voltage levels of the PMTs to 1000 volts and 1050 volts, respectively. This adjustment takes into account the expected performance variability among PMTs of the same model. In long-term measurements using these PMTs operating at elevated voltages, the coincidence count originating from dark current remained consistently below 1 for 1600 s. Thus, the use of two PMTs in coincidence measurements and voltage adjustment effectively addresses the issue of dark current noise and false coincidence events.

The low energy levels of beta rays emitted during tritium decay, typically on the order of a few thousand electron volts, pose a significant challenge to the detection process, as the weak signal is prone to interference from ambient noise. To address this issue, signal processing is necessary to filter out unwanted noise and extract the tritium detection signal. It should be noted that the high-amplitude end of the detector output signal is primarily occupied by high-energy gamma rays and high-energy cosmic particles, which must be filtered out to avoid overwhelming the detector's output signal. Conversely, the low-amplitude end contains a mixture of environmental noise and tritium detection signals, making it crucial to analyze and process these signals separately to avoid potential interference between them. Thus, appropriate signal processing techniques need to be employed to distinguish the tritium detection signal from other signals in the low-amplitude end of the output signal. This can be achieved through careful analysis of the signal spectrum and the application of appropriate filters, such as bandpass filters, to isolate the tritium detection signal. Overall, effective signal processing techniques are essential to ensure accurate and reliable detection of tritium, especially in the presence of ambient noise.

The acquired signal data undergoes processing and analysis using specialized software. The initial step in this process involves applying a filter algorithm to the signal to remove any unwanted noise that may have been captured during acquisition. This step is crucial for ensuring the accuracy and reliability of subsequent signal analysis. Following the application of the filter algorithm, a peak search algorithm is utilized to identify peak signal counts from each photomultiplier tube individually. This information is essential for identifying coincidence events and evaluating system performance. Finally, the coincidence algorithm is employed to optimize the delay time between the two signals and minimize background noise

counts. This algorithm ensures that the signal meets the experiment's requirements and remains unaffected by external factors that could compromise its accuracy. Optimizing the delay time reduces the likelihood of false coincidence events and improves measurement accuracy. Overall, the application of these algorithms significantly enhances the reliability and accuracy of our measurements. It establishes a robust framework for processing and analyzing signal data, enabling us to obtain precise and dependable results.

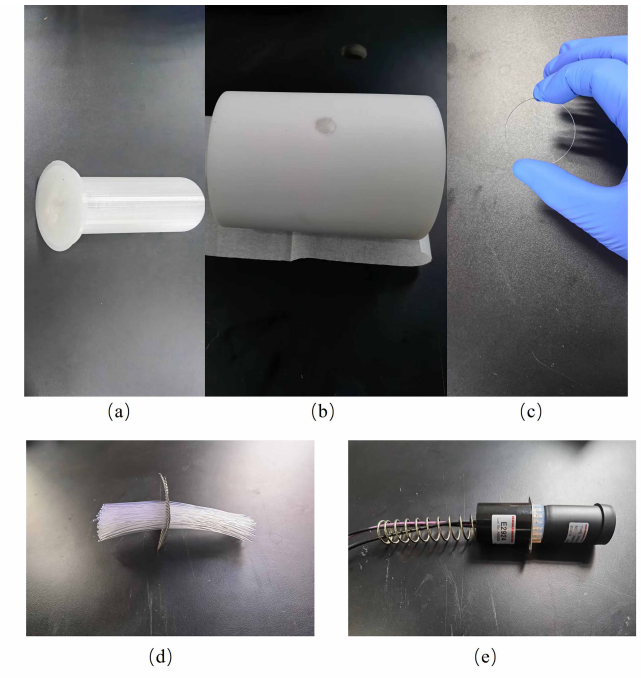

Fig. 5. Physical drawings of the components of the detector: (a) Photomultiplier tube sleeve, (b) the detection chamber, (c) Window of the detection chamber, (d) an array of PSFs, (e) a photomultiplier.

Fig. 5 provides a comprehensive depiction of the various constituent elements comprising the detector system. Figure (a) represents the photomultiplier tube sleeve, which serves the dual purpose of securely holding and shielding the photomultiplier tube against interference noise. Figure (b) showcases the detection chamber, constructed from Teflon material, with dimensions of 90 millimeters in length and 22 millimeters in diameter, matching the size of the photomultiplier tube. The window component of the detection chamber is exemplified in Figure (c), comprising a coated acrylic plate characterized by impressive light transmittance exceeding $95\,\%$. Moving on to Figure (d), it represents an array consisting of 104 plastic scintillation fibers, measuring 100 millimeters in length and 1 millimeter in diameter. The PSF array is meticulously arranged using a hexagonal dense packing configuration, with a spacing of approximately 0.5 millimeters between each PSF. Lastly, Figure (e) represents the photomultiplier itself, specifically utilizing the R3550 model manufactured by Hamamatsu, Japan.

Fig. 6 illustrates a representative distribution of the signal amplitudes obtained from the measurements of the tritium water samples with an activity of $5000\,\mathrm{Bq\,L^{-1}}$. The figure clearly shows that this distribution corresponds to the energy spectrum of beta rays emitted during tritium decay. Due to the 1 millivolt amplitude interval used in the oscilloscope sampling, the tritium energy spectrum distribution could not be completely fitted. The analysis of this spectrum revealed distinct characteristics and allowed the identification of tritium signals amid background noise interference. In the high-energy region of the spectrum (above 0.05 volts), which predominantly consists of signals with higher amplitudes, the presence of background noise interference is more pronounced. The tritium signals in this region are typically minimal and can be easily overshadowed by noise. Consequently, this high-energy region is commonly excluded from tritium signal analysis to ensure accurate and reliable measurements.

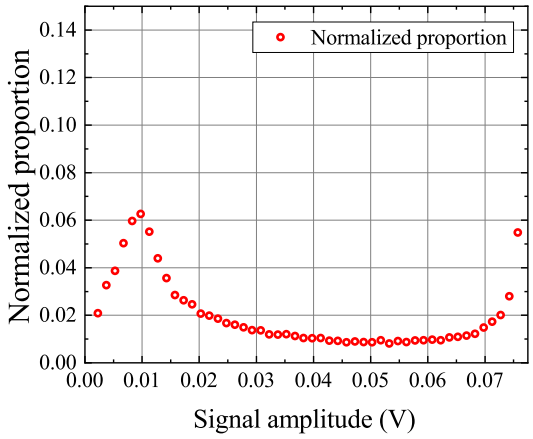

Fig. 6. Typical signal amplitude spectrum measured with the test equipment.

However, special attention was paid to optimizing the signal processing algorithm for the low-energy region (below 0.005 volts) to mitigate the effects of noise interference. The algorithm was fine-tuned to effectively minimize the noise levels in this region, enhancing the sensitivity to low-amplitude tritium signals. A visual examination of Figure 6 demonstrates the effectiveness of this optimization, as it reveals minimal fluctuations or disturbances in the low-energy portion of the spectrum, which is often referred to as a weakened signal burr. By excluding the high-energy region with pronounced background noise interference and applying an optimized signal processing algorithm to the low-energy region, we can focus on accurately detecting and analyzing tritium signals within the spectrum. This approach ensured that our measurements maintained a high level of precision and reliability, enabling us to draw meaningful conclusions from the data.

IV. RESULT AND ANALYSIS

A. Experimental result and minimum detectable activity

After completing the assembly, debugging, and signal algorithm optimization of the equipment, the minimum detectable activity of the equipment was calibrated. The specific parameters of the equipment are as follows: The test equipment employed in this study incorporated a detection array consisting of 104 plastic scintillation fibers, 100 millimeters in length and 1 millimeters in diameter. The PSFs are arranged in a hexagonal dense packing configuration, with a spacing of approximately 0.5 millimeters between adjacent PSFs. This arrangement ensures optimal coverage and sensitivity of the detection system. The detection chamber, in which the PSF array was housed, had a length of 90 millimeters and a diameter of 22 millimeters. This chamber can accommodate a water sample volume of 26.03 milliliters, allowing precise and accurate measurements. To ensure reliable and precise measurements, the experiments were conducted under strict light-avoidance conditions.

Initially, low-background distilled water was introduced into the experimental setup to assess and investigate the background count in the testing environment. The background count is influenced by three primary factors: environmental radiation and noise, supply voltage crosstalk, and the crosstalk count of the photomultiplier. In the absence of adequate lead shielding, the background noise count exhibited fluctuations ranging from 1.12 to 1.25 counts per second during prolonged measurement periods. Consequently, the experiment necessitated multiple measurements to mitigate the influence of background noise on equipment performance. By conducting repeated measurements, we aimed to minimize the impact of background noise and obtain more accurate and reliable experimental data.

Once we determined the experimental method involving multiple measurements, we settled on conducting ten measurements. To ensure the equipment's sensitivity to tritium water with lower activity levels, we employed a descending gradient activity measurement method during the experimental process. This approach systematically evaluated the equipment's capability to detect and quantify tritium water samples with decreasing levels of activity, helping us identify the minimum detectable activity and assess the equipment's performance in effectively capturing and measuring tritium activity even at low levels. For calibration purposes, we used standard tritium water samples to determine the detection efficiency of the equipment. The specific activity of the tritium water samples used in the experiment was calibrated using a liquid scintillation counter (ALOKA LSC-LB7, Japan). Each signal measurement lasted for 1,600 s, and the tritium water samples had specific activities of $935\,\mathrm{Bq\,L^{-1}}$, $4250\,\mathrm{Bq\,L^{-1}}$, and $6200\,\mathrm{Bq\,L^{-1}}$, respectively.

The results obtained from the equipment are depicted in Fig. 7 (a). This figure illustrates a strong positive correlation between the counting rate and the activity of the tritium water sample. As the activity of the tritium water sample increases, the counting rate of the equipment also increases accordingly. The detection efficiency is calculated as the ratio of the actual count of the detector to the theoretical total number of the sample. Based on this correlation, the detection efficiency of the device was calculated to be 1.6×10^{-3}. This detection efficiency is an order of magnitude higher than that of similar detectors used by other researchers, which is 3.11×10^{-4} [24]. The calibration procedure and the determination of the detection efficiency using standard tritium water samples ensure accurate and reliable measurements throughout the study. With the established detection efficiency, subsequent experimental samples' tritium activity levels can be quantified with a high degree of confidence.

To measure low-level radioactivity effectively, it's crucial to minimize the instrument's Minimum Detectable Activity (MDA) as much as possible. MDA typically characterizes the instrument's measurement threshold. The calculation formula for MDA is presented in Eq. (1) [34].

$$MDA = (2.71 + 4.65\sqrt{N_b \times T})/(\varepsilon \times V \times T) \quad (1)$$

where N_b is the background count rate (cps), $\underline{\mathrm{T}}$ is the measurement time (s), ε is the detection efficiency and $\underline{\mathrm{V}}$ is the sample volume (Liter). During the experiment, the measurement duration was set to 1,600 s, the volume of the water sample was precisely measured at 26.03 milliliters, and the instrument exhibited a detection efficiency of 1.6×10^{-3}. The background count rate registered at 1.25 counts per second. Based on these parameters, the minimum detectable activity of the device was calculated as $3165\,\mathrm{Bq\,L^{-1}}$.

Using the experimental results and calculated MDA, we can explore the device's capabilities further. We can calculate the Minimum Detectable Activity (MDA) under varying background noise counts while keeping the measurement time fixed at 1600 s. Additionally, assuming a background noise count of 1.25 cps, we can determine the MDA for different measurement times. This analysis allows us to evaluate the device's performance under different conditions.

To visually depict the MDA change, Fig. 7 (b) and (c) show the MDA curve with a red line. Specifically, Figure (b) emphasizes the substantial enhancement in the device's detection performance due to shielding measures. Additionally, Figure (c) illustrates variations in the device's performance at different measurement times during practical use. These fluctuations underscore the device's stringent detection performance requirements, especially in short-term measurements where precision and effectiveness are paramount.

The absence of a lead shielding layer in the experimental setup resulted in a noticeable increase in background noise count. While this might have somewhat mitigated noise impact when measuring highly active tritium water samples, it's important to note that for low-activity tritium water measurement, a lead shielding layer is crucial. Adding a lead shielding layer can significantly enhance detector performance, reducing minimum detectable activity and improving overall accuracy. Given this result, it's highly advisable to include a lead shielding layer in future experiments. This shield acts as a protective barrier, effectively reducing external interferences and minimizing background noise count. Thus, the de-

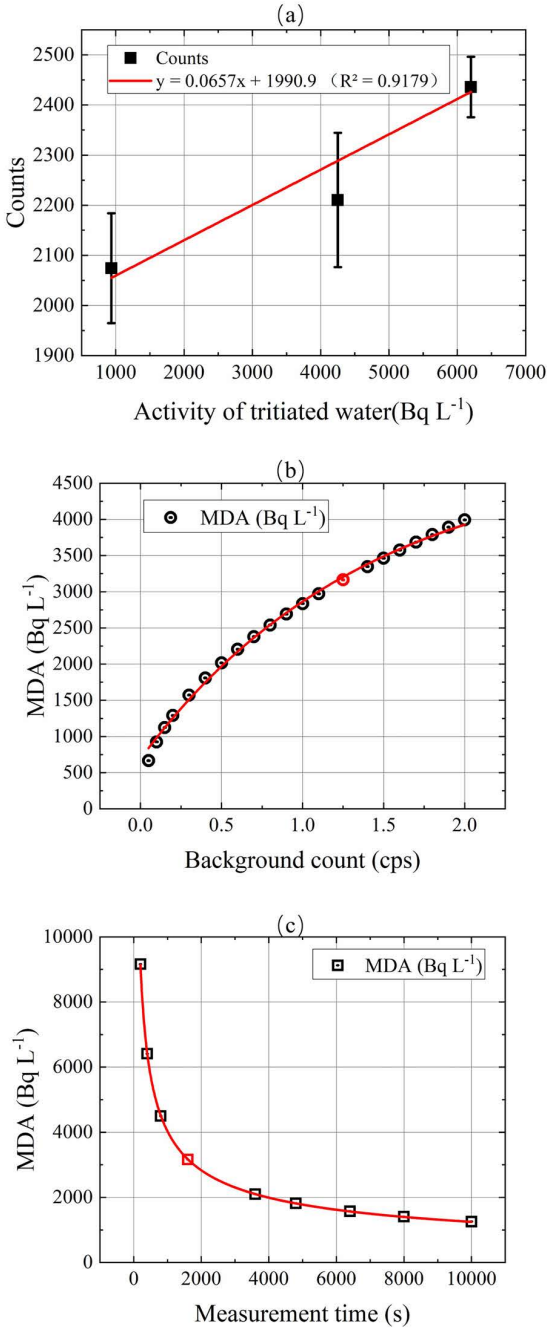

Fig. 7. Experimental results and Evaluation of the minimum detectable activity (MDA): (a) Experimental results, (b) background count rate and MDA when the measurement time is 1600 s, (c) measurement time and MDA, the red symbols are the performance confirmed by the test device in this study.

tection system will be better equipped to accurately measure and quantify low levels of radioactivity in tritium water samples. Incorporating a lead shielding layer not only enhances detector sensitivity and precision but also ensures reliable and reproducible results. Therefore, for more robust and accurate measurements of low-activity tritium water samples, it is essential to include a lead shielding layer in future experimental setups.

B. Analysis of experimental results and outlook

The device's detection efficiency was calculated to be 1.6×10^{-3}, while the simulation result for the entire detection system is 4×10^{-4}. The actual equipment's detection efficiency is approximately four times higher than that of the simulated equipment. This significant difference can be attributed to two main reasons. Firstly, inaccurate simulation results of low-energy β rays in the model led to a substantial systematic deviation in the results. Additionally, the actual PSF exhibits a certain arc, increasing the contact volume with the water body and resulting in higher detection efficiency compared to the simulation results. However, it's important to note that simulation results are generally instructive. Currently, the existing device is in the initial stage of development. With a measurement time of 1600 s, it achieves a minimum detectable activity of $3165\,\mathrm{Bq\,L^{-1}}$. The water sample volume is 26.03 milliliters, and the sample injection process can be completed within 10 s using a peristaltic pump. Consequently, it can function as a warning measurement device for high-activity tritium water samples, suitable for alarm systems in nuclear power plants and other specialized facilities. The simulation results indicate that increasing the number of plastic scintillation fibers can positively impact both the detection efficiency and volume of the entire system. Additionally, extending the length of the PSF contributes to an increase in the detection volume. Reducing the diameter of the PSF allows for a higher density of PSFs within the same area, thereby enhancing the detection efficiency by augmenting the detection volume. To further improve detection performance, strict shielding methods can be implemented to effectively control the background noise count. Many detection devices have successfully achieved a background noise count between 0.01 and 1 count per second, or even lower. By employing rigorous shielding measures to eliminate interference from ambient noise counts and restrict the background noise count to below 0.1 cps, the equipment's detection performance can be significantly enhanced. This reduction in background noise count also leads to a decrease in the minimum detectable activity of the device. Based on the above conditions and simulation results, it is predicted that with a measurement time set at 1600 s, the MDA of the device will be below $50\,\mathrm{Bq\,L^{-1}}$. Notably, China mandates that the concentration of tritium in water 1 km downstream of inland nuclear power plants should not exceed $100\,\mathrm{Bq\,L^{-1}}$, while the European Council Directive 2013/51/Euratom requires a maximum tritium level in water for human consumption to be lower than $100\,\mathrm{Bq\,L^{-1}}$. We are actively engaged in refining the equipment and conducting experiments to validate the accuracy of the inferred results. With such exceptional performance, the device can effectively monitor tritium content in both nuclear power plant discharge outlets and common drinking water sources, enabling early warning measurements.

V. SUMMARY

In this study, we designed, simulated, and developed a tritium monitoring device incorporating a PSF array. To validate its performance, we conducted experimental tests to determine its detection efficiency and minimum detectable activity. The recorded detection efficiency of the device was 1.6×10^{-3}, four times higher than the theoretical simulation value of 4×10^{-4}. However, we explained this discrepancy, emphasizing the importance of simulations in guiding the research and development of the device.

Without shielding, the device showed a minimum detectable activity of $3165\,\mathrm{Bq\,L^{-1}}$ over a 1600-second measurement period. However, simulation results suggested that by lengthening the PSF, increasing their quantity, and implementing rigorous shielding measures, the device's minimum detectable activity could improve to $50\,\mathrm{Bq\,L^{-1}}$ within the same timeframe. Moreover, by using smaller diameter PSFs along with optimized shielding and signal processing algorithms to enhance detection efficiency, the device's minimum detectable activity could be further reduced. This significant progress underscores the device's potential for widespread application in tritium monitoring.

Overall, our study successfully designed and developed a tritium monitoring device based on a PSF array. Experimental validation and simulation results showed the device's capability to achieve desirable levels of minimum detectable activity through various optimization strategies. These results underscore the promising prospects and broad applications of the device in the field of online tritium monitoring in water.

[1] G.Q. Jiang. Tritium and Tritium Engineering Technology. (National Defense Industry Press, 2007), pp. 14–22. (in Chinese)

[2] L.L. Qin, Z.Q. Dai Z, Z.H. Xia et al., Evaluation of Dose Derived from HTO for Adults in the Vicinity of Qinshan Nuclear Power Base. Health Phys. C. **117**, 443–448 (2019). doi:10.1097/HP.0000000000001072

[3] W.Y Cheng, J. Liang, M.J. Zhang et al., Radiation Dose Assessment of Tritium Released from the Thorium Molten Salt Reactor. Nuclear Science and Engineering. **197**, 1534–1544 (2023). doi:10.1080/00295639.2022.2158020

[4] Q.S. Xu, L.L. Qin, Xia Z, W. Liu et al., Distribution of atmospheric multi-forms tritium in the vicinity of Qinshan nuclear power plants. Nucl. Tech. **42**, 1–6 (2019). (in Chinese) doi:10.11889/j.0253-3219.2019.hjs.42.070601

[5] F. Bin, B. Chen, W.H Zhuo et al., Seasonal and Spatial Distribution of Atmospheric Tritiated Water Vapor in Mainland China. Environ Sci Technol. **53**, 14175–14185 (2019). doi:10.1021/ACS.EST.9B03855

[6] J. Liang, L. Du, W.Y. Cheng et al., Distributions of tritium with different chemical form in the soil around Qinshan Nuclear Power Plant. J Radioanal Nucl Chem. **328**, 1153–1159 (2021). doi:10.1007/S10967-021-07720-0

[7] J. Liang, W.Y. Cheng, J.L. Lin et al., Distribution of hydrogen isotope in the soil around the Qinshan Nuclear Power Plant. J Environ Radioact. **263**, 107170 (2023). doi:10.1016/J.JENVRAD.2023.107170

[8] Q. Zhang, L. Du, Z.Q Dai et al., Studies of particle size distribution of Non-Exchangeable Organically Bound Tritium activities in the soil around Qinshan. Nuclear Power Plant. J Environ Radioact. **192**, 362–367 (2018). doi:10.1016/j.jenvrad.2018.07.004

[9] B.J. Nie, S Fang, M Jiang et al., Anthropogenic tritium: Inventory, discharge, environmental behavior and health effects. Renewable and Sustainable Energy Reviews. **135**, 110188 (2021). doi: 10.1016/j.rser.2020.110188.

[10] E. Furuta, N. Iwasaki, Y. Kato et al., A new tritiated water measurement method with plastic scintillator pellets. Isotopes Environ Health Stud. **52**, 560–566 (2016). doi:10.1080/10256016.2015.1133618

[11] C. Varlam, I. Stefanescu, OG. Duliu et al., Applying direct liquid scintillation counting to low level tritium measurement. Appl Radiat Isot. **67**, 812–816 (2009). doi:10.1016/J.APRADISO.2009.01.023

[12] F. Priester, M. Klein. TRitium Activity Measurements with a PhotomultipliEr in Liquids–The TRAMPEL experiment. Fusion Eng Des. **109-111**, 1356–1359 (2016). doi:10.1016/J.FUSENGDES.2015.12.027

[13] R.A. Sigg, J.E. McCarty, R.R. Livingston et al., Real-time aqueous tritium monitor using liquid scintillation counting. Nucl. Inst. Meth. A. **353**, 494–498 (1994). doi:10.1016/0168-9002(94)91707-8

[14] B. Arun, I. Vijayalakshmi, K. Sivasubramanian et al., Optimization of Liquid Scintillation Counter for Tritium Estimation in Water Samples. Radiochemistry. **61**, 61–65 (2019). doi:10.1134/S1066362219010090

[15] Z.L. Chen, S.X. Xing, H.Y. Wang et al., The effect of vial type and cocktail quantity on tritium measurement in LSC. Appl. Radiat. Isot. **68**, 1855–1858 (2010). doi:10.1016/J.APRADISO.2010.04.015

[16] F. Verrezen, H. Loots, C. Hurtgen. A performance comparison of nine selected liquid scintillation cocktails. Appl. Radiat. Isot. **66**, 1038–1042 (2008). doi:10.1016/j.apradiso.2008.02.050

[17] J.L. Erchinger, J.L. Orrell, C.E. Aalseth et al., Background characterization of an ultra-low background liquid scintillation counter. Appl. Radiat. Isot. **126**,168–170 (2017). doi:10.1016/J.APRADISO.2017.01.032

[18] K.J. Hofstetter, H.T. Wilson. Aqueous effluent tritium monitor development. Fusion Technol. **21**, 446–451 (1992). doi:10.13182/fst92-a29786

[19] T. Kawano, T. Uda, T. Yamamoto et al., Tritium water monitoring system based on CaF2 flow-cell detector. Fusion Sci. Technol. **60**, 952-955 (2011). doi:10.13182/FST11-A12573

[20] T. Kawano, H Ohashi, Y. Hamada et al., Comparative testing of various flow-cell detectors fabricated using CAF2 solid scintillator. Fusion Sci. Technol. **67**, 404–407 (2015). doi:10.13182/FST14-T39

[21] Y. Hatano, M. Hara, H. Ohuchi-Yoshida et al., Measurement of tritium concentration in water by imaging plate. Fusion Eng. Des. **87**, 965–968 (2012). doi:10.1016/j.fusengdes.2012.02.057

[22] F. Priester. A New Device for Activity Measurement of Tritiated Water. Fusion Sci. Tech. **71**, 600–604 (2017). doi:10.1080/15361055.2017.1289585

[23] E. Furuta, N. Iwasaki, Y. Kato et al., A new tritiated water measurement method with plastic scintillator pellets. Isotopes Environ. Health Stud. **52**, 560–566 (2016).

doi:10.1080/10256016.2015.1133618
[24] Y. Sanada, T.Abe, M. Sasaki et al., Basic study on tritium monitor using plastic scintillator for treated water discharge at Fukushima Daiichi Nuclear Power plant. J Nucl. Sci. Technol. **61**, 693–702 (2024). doi:10.1080/00223131.2023.2258880
[25] C. Azevedo , A. Baeza, M. Brás et al., TRITIUM - A Quasi Real-Time Low Activity Tritium Monitor for Water. EPJ Web Conf. **225**, 03008 (2020). doi:10.1051/epjconf/202022503008
[26] W.H. Lv, H.C. Yi, T.Q. Liu et al., Gross beta determination in drinking water using scintillating fiber array detector. Appl. Radiat. Isot. **137**, 161–166 (2018). doi:10.1016/j.apradiso.2018.04.007
[27] P. Truscott, F. Lei, C. Dyer et al., Geant4 - a new Monte Carlo toolkit for simulating space radiation shielding and effects. IEEE Radiat. Eff. Data Work. 147-152 (2000). doi:10.1109/REDW.2000.896281
[28] S. Agostinelli, J. Allison, K. Amako et al., Geant4—a simulation toolkit. Nucl. Instrum. Meth. A **506**, 250-303 (2003). doi:10.1016/S0168-9002(03)01368-8
[29] J. Allison, K. Amako, J. Apostolakis et al., Geant4 developments and applications. IEEE Trans. Nucl. Sci. **53**, 270-278 (2006). doi:10.1109/TNS.2006.869826
[30] R.Y. Xu, C.H. Dong, X.Q. Mao et al., Simulation results of the online tritiated water measurement system. Nucl. Sci. Tech. **32**, 1–9 (2021).doi:10.1007/S41365-021-00964-1
[31] C.H. Dong, K.Y. Liao, R.Y. Xu et al., Design and preliminary test of tritiated water online detector system based on plastic scintillators. Nucl. Sci. Tech. **33**, 1–11 (2022). doi:10.1007/s41365-022-01115-w
[32] H.K. Wu, C. Li. A ROOT-based detector test system. Nucl. Sci. Tech. **32**, 115 (2021). doi:10.1007/S41365-021-00952-5
[33] P, Juyal,K.L.Giboni, X.D. Ji et al.,On proportional scintillation in very large liquid xenon detectors. Nucl. Sci. Tech. **31**, 1–8 (2020). doi:10.1007/S41365-020-00797-4
[34] L.A. Currie. Limits for Qualitative Detection and Quantitative Determination: Application to Radiochemistry. Anal. Chem. **40**, 586–593 (1968). doi:10.1021/ac60259a007